A Geometric Approach to Predicting and Reducing Land Contamination in Coastal Altimetry Signals

Chris Green[1,2], J Derek Fairhead[1,2], Kirsten Fletcher[1],
[1]GETECH, Elmete Lane, Leeds, LS8 2LJ,UK.; [2]University of Leeds LS2 9JT, UK.

DATA

GETECH

Introduction

Extracting altimeter signal from coastal areas is challenging for a number of reasons, but the only issue that is unique to the coastal region is contamination of altimeter signal by reflection or diffraction from land topography. As illustrated in Figure 1, the contamination depends on the height of the topography and the offset from the altimeter position.

In this study we have attempted to use a simple geometric approach to map the areas of contamination based on available DEM data. This can be achieved over large areas, but is dependent on the DEM data available. For the purpose of this study we assume that our interest is in using the altimeter data to generate high-resolution gravity products and increase their confidence close to the coast. For his reason, we will only consider contamination at the leading edge of the altimeter waveforms. Moreover, we will only consider data sets with high spatial resolution and hence have exclusively considered ERS-1 Geodetic Mission data.

We have also considered how the same geometric approach might help to remove the effects of diffracted signals from onshore topography. This requires devising a model of the expected noise signals; several such signals have been identified in the data and first attempts have been made to reduce their effect.

Figure 1. Effect of land contamination on satellite altimeter data. As the satellite approaches the coast the likelihood and the impact of land contamination increases.

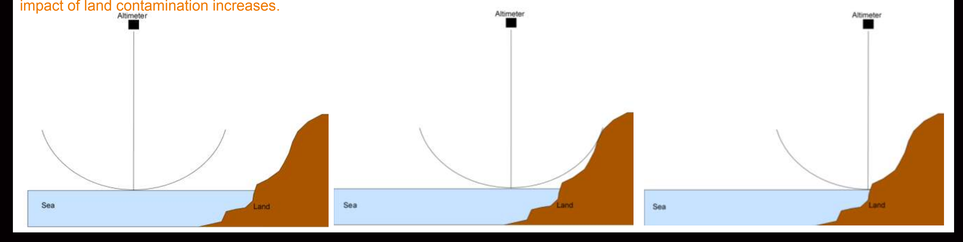

Topographic Prediction of Contamination

Approach

Diffractions from land topography have been observed for small islands and promontories (Gommenginger et al., 2011); similar diffractions due to ships have also been observed (Tournadre, 2007). Here, we wish to study how far such diffractions might interfere with the altimeter signal generally. The apparent height h_{app} of the land is related to its actual height h and the distance dx to the satellite location by:

$$h_{app} = h - \frac{dx^2}{2H} - \frac{dx^2}{2R}$$

where H is the height of the satellite and R is the radius of the Earth. To avoid possible contamination, the reflection must arrive after the leading edge of the waveform. This leading edge might typically extend over two gates forward and backward and hence to avoid contamination h_{app} must be less than -1 m.

For this purpose, we have used SRTM 250 m grids generated by CGIAR (Jarvis et al., 2008). These grids have the advantage that holes have been infilled and hence they are continuous onshore. The horizontal resolution is not optimum (although 90 m grids are also available), but the lack of precision in the heights (quoted to 1 m) limits what might be attempted with the data.

It has been noted (Brooks et al., 1990, Brooks et al., 1997) that contamination from land depends not only on the elevation of the land, but also on the slope. Specular reflections are likely to have the biggest impact on the satellite waveforms due to their amplitude. Specular reflections require the reflecting surface to be smooth on the order of the wavelength of the signal (a few cm) and normal to the altimeter signal (small slopes up to ~1); the surface needs also to be flat over some distance, although the observation of reflections from ships or parts of ships (Tournadre, 2007) suggests that this extent can be quite small. Such surfaces may well be quite common in nature, but the available DEM is inadequate to model them due mainly to the limited vertical precision. A higher precision DEM could allow a Kirchhoff-Helmholtz integration (or summation), which would treat specular and diffuse reflections together, but the precision of the DEM makes it impractical to calculate wave effects in such detail. Statistical descriptions of the sea surface can be used to predict reflection behaviour and although that may be difficult for land topography in general, it could be feasible for some terrain types. In any case, the contamination predicted by this approach is likely to be the worst case scenario.

The maximum distance for land contamination depends on the width of the altimeter beam as well as the surface topography. A radius of ~9 km at half amplitude is predicted from instrument design (Quartly et al., 2001). A radius of ~12 km might be estimated based on statistics of successful ocean retracking (Gommenginger et al., 2011). However, a radius of 20+ km is predicted by observations of land contamination by Deng et al. (2002). Hence in this study, we use a radius of 25 km, so that we can compare with the results of Deng et al. (2002) and for that reason our study has focused on Australia. Figure 2 shows the area that would be potentially impacted around Tasmania; for statistical analysis pseudo-tracks in an ERS-1 Geodetic Mission pattern have been used.

Results

Figure 3 shows the values of the apparent height h_{app} for all pseudo tracks around Australia. In Figure 3a the heights are plotted against the distance from the identified diffraction point; for this reason, the smooth parabolic shapes expected from diffraction dominate the plot. In Figure 3b the heights are plotted against the distance to the nearest coast; this is considered to be the more useful comparison, but the clean parabolic shapes are lost due to tracks not running perpendicular to the topography. The blue line shows the limiting case of zero topographic elevation whilst the red line shows the cut-off for contamination. Clearly there are many more potentially contaminated points (above the red line) at small distances from the coast, whilst at large distances most points are uncontaminated (below the red line).

Table 1 shows our results compared to those of Deng et al. (2002) divided into the same 15 x 15 squares and using a table format based on that in Deng et al. (2002). Not all columns are comparable; for example we have calculated the minimum uncontaminated distance in each square and the median as well as the mean contaminated distance. It is clear that the parameters vary from square to square, depending upon the coastal topography. Of the parameters which are comparable, the values for maximum contaminated distance in each square are roughly the same for each approach, although there is no correlation in the variation from square to square. The values for mean contaminated distance, however, are significantly different with our values generally ~2 km less than those of Deng et al. (2002). Given that our values should represent the worst case scenario, this seems to suggest that some of the land contaminated signals identified by Deng et al. (2002) are not actually contaminated by land, but disturbed by some other process.

The 50% contamination distance is the distance at which 50% of the waveforms are potentially contaminated by land. Values in Table 1 are based on the histograms shown in Figure 4. This parameter is representative of typical limits for contamination within an area. Figure 4 also shows 50% contamination distances calculated for 1 x 1 squares; these show a large range of values dependent on coastal topography, which represent a range of topographic effects.

Table 1. Statistical comparison of potential contamination derived from DEM against results published by Deng et al. (2002).

		Topo considerations - 25 km radius					Deng et al., 2002			
Long	Lat	Min unaffected dist (km)	Max affected dist (km)	Mean affected dist (km)	Median affected dist (km)	50% affected dist (km)	Max affected dist (km)	Mean affected dist (km)	Max depth (m)	Coastal types
120E-135E	15S-0S	2.17	14.79	2.56	2.08	4.84	19.39	6.92	52.9	Rocks, reefs and small barrier reefs
135E-150E	15S-0S	1.74	20.62	3.96	3.10	5.18	19.68	6.75	43.2	Small and large barrier reefs
105E-120E	30S-15S	1.71	18.88	3.46	2.67	4.48	21.51	6.18	336.9	Dune rocks, cliffs, and low-gradient beaches
120E-135E	30S-15S	1.78	12.49	2.28	1.75	5.35	19.20	7.79	48.9	Low gradient beaches
135E-150E	30S-15S	1.71	23.38	5.44	3.85	8.58	19.07	7.78	44.4	Small and large barrier reefs
150E-165E	30S-15S	1.70	15.88	4.64	3.84	8.47	11.99	8.67	12.2	Large barrier reefs
105E-120E	45S-30S	2.69	22.17	5.79	4.97	10.62	20.62	7.94	361.5	Dune rocks, cliffs, and sandstone reefs
120E-135E	45S-30S	1.97	16.68	4.39	3.82	7.42	19.07	6.98	88.5	Dune rocks, mudflats, cliffs, and sand beaches
135E-150E	45S-30S	2.36	23.35	5.69	4.50	9.34	21.76	7.30	361.2	Rock shores, reefs, sandy and rugged beaches
150E-165E	45S-30S	4.85	21.55	6.19	5.58	12.52	8.02	2.07	178.7	Rocks and large barrier reefs
	Mean	2.27	18.98	4.44	3.62	7.68	18.03	6.84		

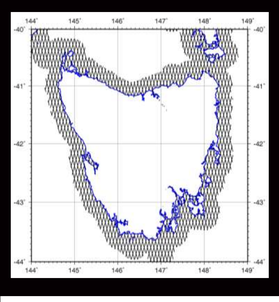

Figure 2. The area of potential land contamination around Tasmania. Pseudo-tracks of ERS-1 Geodetic Mission data have been windowed to within 25 km of the coast.

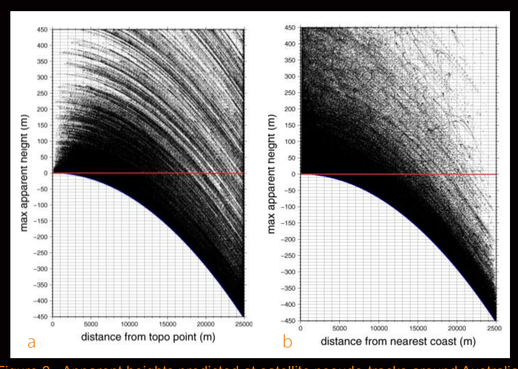

Figure 3. Apparent heights predicted at satellite pseudo-tracks around Australia based on a 250 m DEM. When plotted against distance from point diffractor (a), parabolic shapes can be observed throughout; plotting against distance from the coast (b) is more representative, but more complex. Blue curve is the limit for zero topography; red line is the cut-off for contamination of the leading edge of the altimeter waveform – potentially contaminated above the line.

Figure 4. Distance for 50% contamination shown for 1° x 1° squares around Australia. Histograms show potentially contaminated (red) and non-contaminated (green) signals for each 15° x 15° square.

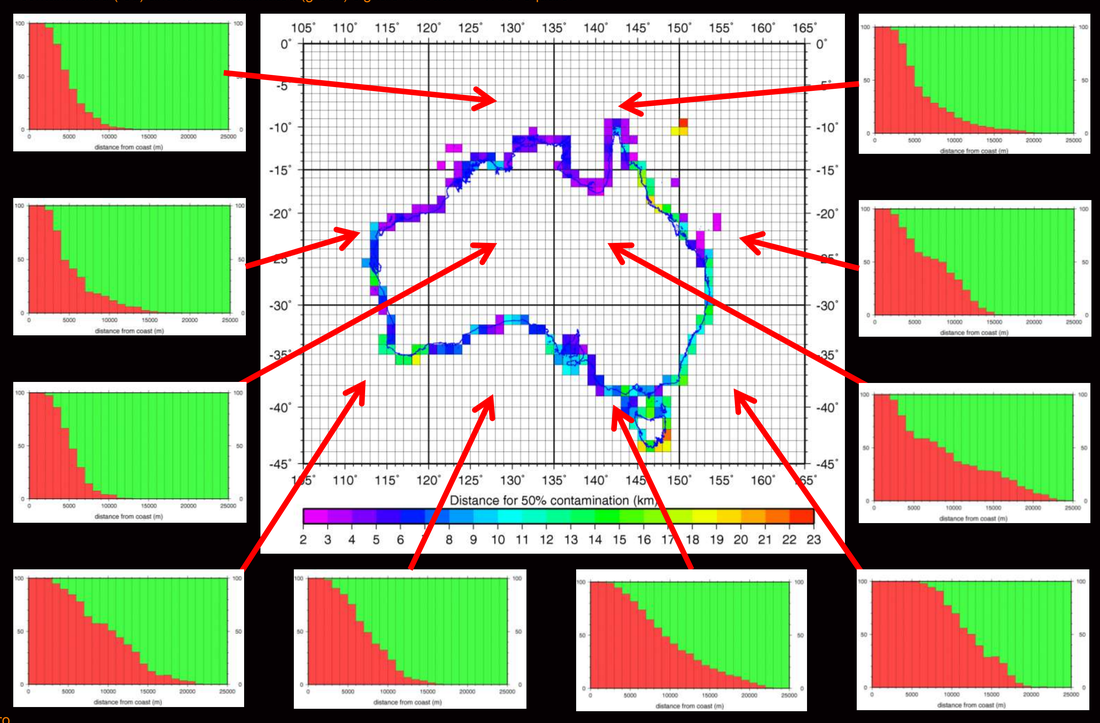

Attempted Waveform Cleaning

Land altimeter reflections and land contamination of marine reflections are part of the same system, such that if we plot the nearshore and coastal waveforms together they should show coherent signals. If these signals can be predicted and modelled, then there is the potential to remove anomalous diffractions and improve the retracking of sea surface reflections.

Figure 5 shows the locations of three ERS-1 satellite tracks in the Bass Strait area, which show predicted patterns. These are shown in Figures 6, 7 and 8a:

- Figure 6 shows descending track u18051 as it reaches the coast of Tasmania. This is a relatively high relief coastal area and consequently a series of diffractions from land sources can be seen at the end of the profile as well as a diffraction from near the coast.
- Figure 7 shows ascending track v15059 as it reaches the coast of Cape Barren Island. This shows a clear diffraction from near the coast.
- Figure 8a shows ascending track v18001 as it reaches the coast of Victoria.

The waveforms in these figures have been re-aligned to their proper geometric position to remove shifts of the recording window due to previous early arrivals (Brooks et al., 1997). It should also be noted that the shape of diffractions is the same whether the source is on the profile or off to one side; thus it is quite feasible to have a diffraction whose apex appears slightly offshore as measured along the profile.

Cleaning up diffractions is a similar problem to seismic migration – except that in this case the collapsed signal needs to be removed rather than kept. Seismic migration algorithms are many and complex and as an initial investigation we will apply a simpler approach to track v18001.

The area of the track displaying the diffraction has been windowed and a normal moveout (NMO) correction has been applied – Figure 8b. The NMO correction is only valid for diffractions at the along track location of the apex of the diffraction parabola, but it is equally applicable to diffractors at any height or at any distance perpendicular to the profile. Due to the large distance to the altimeter, the same adjustment is applicable for all points along the waveform and there is no signal stretch as would be observed in seismic NMO. In Figure 8b the ocean reflection signal now forms a parabola and the point diffraction signal is now close to horizontal. The fact that the diffraction signal is not totally horizontal and has significant width at the centre could be indicative of a more complex diffraction than would be predicted from a single point – maybe summed diffractions from a set of nearby topographic points.

Linear features on the NMO adjusted data set can be removed in the Fourier (FK) domain based on their strike. Figure 8c shows the data set after a few strike filters have been applied to remove linear signals. The removal of the primary diffraction is far from complete; its large amplitude relative to the sea surface reflections makes this a very difficult process. Figure 8d shows the strike filtered data set re-adjusted and patched (crudely) into the original waveform pattern. Some interfering signals have been reduced or removed (compared to Figure 8a) but such removal is insufficient to allow any more sea surface reflections to be retracked.

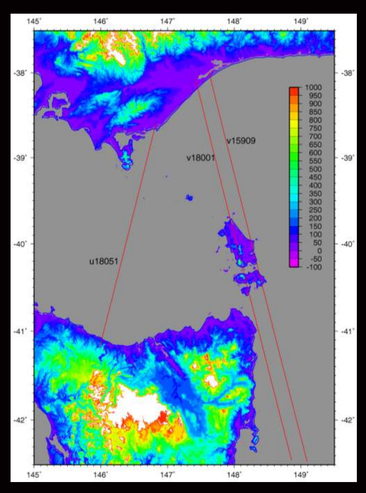

Figure 5. Three ERS-1 satellite profiles in the Bass Strait which show diffractions near the coast.

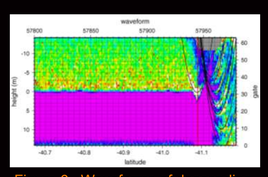

Figure 6. Waveforms of descending ERS-1 track u18051 as it reaches the northern coast of Tasmania. Black lines show theoretical diffraction parabolas; red line shows the location of the coastline along the track.

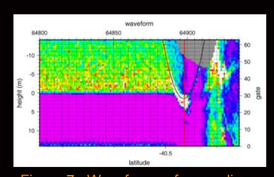

Figure 7. Waveforms of ascending ERS-1 track v15059 as it reaches the southern coast of Cape Barren Island. Black line shows theoretical diffraction parabola; red line shows the location of the coastline along the track.

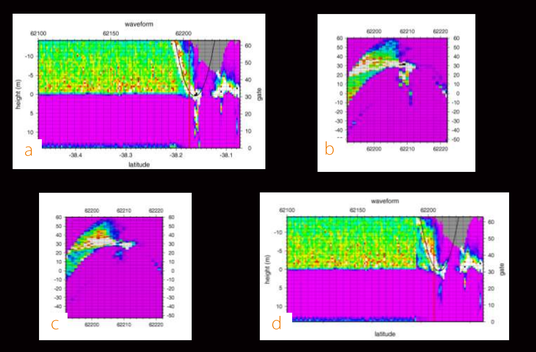

Figure 8. Waveforms of ascending ERS-1 track v18001 as it reaches the southern coast of Victoria (a) in original form, (b) a subset after NMO adjustment, (c) NMO adjusted subset after strike filtering, (d) with strike filtered subset patched back in.

Conclusions

Topographic grids have successfully been used to identify areas potentially contaminated by land signals. This can still be reliably achieved even using a DEM that is inadequate for waveform modelling. The results vary significantly by geographic area and the extent of land contamination in a given area can be predicted.

The worst case scenario approach used here has results which differ significantly to contamination observed from actual waveform data. This suggests that land contamination previously identified may actually be disturbance from other sources. This in turn suggests that land contamination is less of an issue than previously thought (although still significant close to the coast); other problems may, however, have a greater extent.

Land based diffractions observed in real waveform data appear to fit the theoretical parabolic shape. An attempt to use this geometry to remove diffractions and image more sea surface reflections has not been successful; the large amplitude of the land contaminated signal remains a significant problem in this approach. However, more sophisticated seismic migration algorithms may yet generate better results.

References

BROOKS, R. L., LOCKWOOD, D. W. & HANCOCK, D. W., III (1990) Effects of Islands in the Geosat Footprint. *J. Geophys. Res.,* 95, 2849-2855.

BROOKS, R. L., LOCKWOOD, D. W., LEE, J. E., HANCOCK, D. W., III & HAYNE, G. S. (1997). *Land Effects on TOPEX Radar Altimeter Measurements in Pacific Rim Coastal Zones*. Available at: http://topex.wff.nasa.gov

DENG, X., FEATHERSTONE, W. E., HWANG, C. & BERRY, P. A. M. (2002) Estimation of Contamination of ERS-2 and POSEIDON Satellite Radar Altimetry Close to the Coasts of Australia. *Marine Geodesy,* 25, 249-271.

GOMMENGINGER, C., THIBAUT, P., FENOGLIO-MARC, L., QUARTLY, G., DENG, X., GÓMEZ-ENRI, J., CHALLENOR, P. & GAO, Y. (2011) Retracking Altimeter Waveforms Near the Coasts: A Review of Retracking Methods and Some Applications to Coastal Waveforms. in VIGNUDELLI, S., KOSTIANOY, A., CIPOLLINI, P. & BENEVISTE, J. (Eds.) *Coastal Altimetry.* pp. 61-101. Heidelberg, Springer.

JARVIS, A., REUTER, H. I., NELSON, A. & GUEVARA, E. (2008) Hole-filled Seamless SRTM Data V4. INTERNATIONAL CENTRE FOR TROPICAL AGRICULTURE (CIAT). Available at: http://srtm.csi.cgiar.org

QUARTLY, G. D., SROKOSZ, M. A. & MCMILLAN, A. C. (2001) Analyzing Altimeter Artifacts: Statistical Properties of Ocean Waveforms. *Journal of Atmospheric and Oceanic Technology,* 18, 2074-2091.

TOURNADRE, J. (2007) Signature of Lighthouses, Ships, and Small Islands in Altimeter Waveforms. *Journal of Atmospheric and Oceanic Technology,* 24, 1143-1149.

UNIVERSITY OF LEEDS